FINAL REPORT

Contract NAS8-34957
MCT CRYSTAL GROWTH

by

Professor James K. Baird

Prepared for

National Aeronautics and Space Administration
George C. Marshall Space Flight Center
Marshall Space Flight Center, Alabama 25812

Submitted by

The University of Alabama in Huntsville
School of Mathematics and Natural Sciences
Huntsville, Alabama 35899

February 23, 1988

Report on DTA Furnace

Hai-Yuin Cheng
September 25, 1987

The Sample

The $Hg_{1-x}Cd_xTe$ alloy with x = .1 was prepared by reacting the constituent elements in a sealed, fused-silica, 5-mm i.d. and 10-mm o.d. ampoule.

The ampoule was cleaned with aqua regia, distilled water, acetone and then methanol, and was baked at 1000 C in a vacuum of 500 torr (the best available, better than no vacuum).

The ampoule was then loaded with 1.7835 g Hg first, then 1.234 g Te, and finally .108 g Cd, then evacuated to about 10^{-2} torr and sealed-off.

The sealed ampoule was put in the rocking-furnace. The furnace was heated up from room temperature to 760 C (the actual temperature is about 90 C higher than this reading from the programmable controller) in 10 hours. the furnace was rocking while the temperature was held at 760 C for 17 hours, then the power and rocking motor were turned off. The ampoule was pulled out of the furnace at 520 C.

The Antimony Reference

The ampoule used for the reference was identical to that used for the sample. The ampoule was cleaned with aqua regia, distilled water, acetone, and then methanol, and then baked from room temperature to 1050 C at 10^{-7} torr.

The ampoule was then loaded with 2.6552 g Sb (same volume as the HgCdTe sample), then evacuated to about 10^{-2} torr. The antimony was melted with a torch, then the ampoule was sealed-off. Both the sample and reference ampoules were shortened a bit by Robbie to reduce the free volume.

Temperature Profile

The Marshall platinum-wound tubular furnace is mounted vertically. A quartz tube of 30-mm o.d. and 27-mm i.d. is filled with fiberfrax and is placed inside a metal tube as shown in the figure.

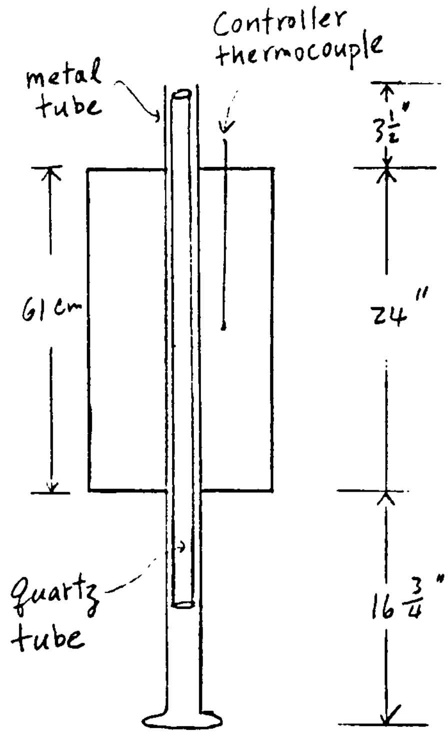

First the temperature profiles at setpoints 650, 900 and 1100 C were measured with a type-K thermocouple. As shown in the plots. x is measured from the bottom of the furnace. and the furnace is 24 inches (61 cm) long. Since the peaks of the profiles were not consistent, the thermocouple was replaced by a type-R thermocouple. Although the profiles were consistent, the peak was off center. It was displaced toward the top of the furnace by about 3 cm. The flat zone is about 3 cm at 1100 C.

At lower set points the flat zone broadens slightly, being 4 to 5 cm at 900 C and about 7 cm at 650 C.

While the sample and reference were being prepared, the temperature profiles described below were measured at a setpoint of 900 C. The intention was to find a way to broaden the flat zone. A schematic diagram of the furnace and its taps is shown below.

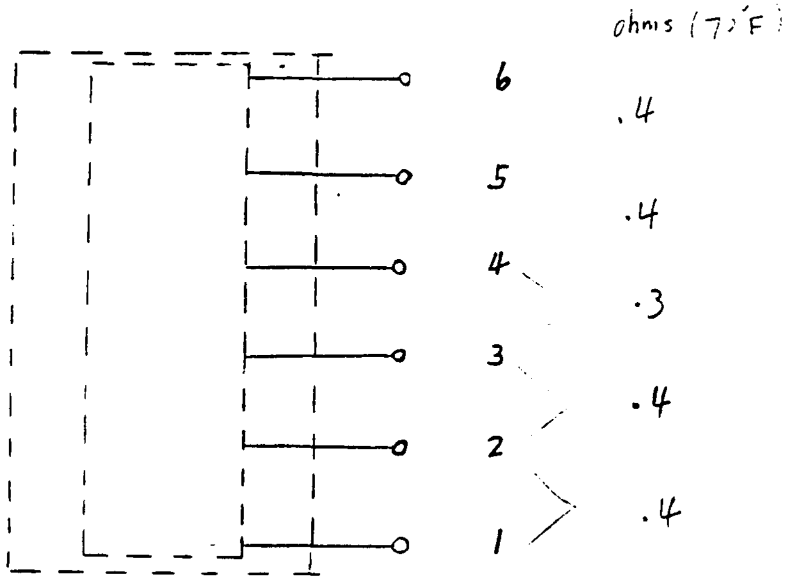

a) Shunt between external binding posts 2 and 4 with a resistance 11, 7.4 and 3.5 ohm respectively. As shown in the plots, putting the shunt between taps 2 and 4, makes the profile more peaked, and reduces the breadth of the flat zone.

b) Shunt between taps 3 and 4 with a resistance 3.5, 0.9, 0.4 and 0 (shorted) ohm respectively. From the plots, it shows that shunting the center zone (taps 3 and 4) had no effect upon the breath of the flat zone except for shifting it to the geometrical center of the furnace. The flat zone is essentially the same with and without a shunt.

c) Several attempts were made to broaden the flat zone by shunting taps 4 & 5 and 2 & 3, in addition to (b), but these efforts resulted in asymmetric profiles which were quite unexpected. It is possible that these complications result from convection in the vertical orientation or from some peculiarity in the windings.

ORIGINAL PAGE IS
OF POOR QUALITY

Hg(1-x) Cd(x) Te

```
x          =    0.100
DENSITY    =    7.860   g/cm**3
MOLES Te   =    0.010
VOLUME     =     .4     cm**3
DIAMETER   =    0.50    cm
LENGTH     =    2.0     cm
  STOCHIOMETRIC MASSES ARE
MERCURY         1.7449 g
CADMIUM          .1086 g
TELLURIUM       1.2332 g

TIME    9:31
DATE   SEPTEMBER 1,1987
```

Hg MASS CALCULATION

```
x          =    0.100
DENSITY    =    7.860   g/cm**3
MOLES Te   =    0.010
FREE VOL   =     .8     cm**3
DIAMETER   =    0.50    cm
LENGTH     =    4.0     cm
  STOCHIOMETRIC MASSES ARE
MERCURY         1.7450 g
CADMIUM          .1086 g          .108
TELLURIUM       1.2332 g          1.234

EXCESS Hg        .0428 g
TOTAL  Hg       1.7878 g          1.7835

ACCEPTABLE RANGE OF Hg MASS

   1.7771 g to   1.7878 g

TIME    9:32
DATE   SEPTEMBER 1,1987
```

$\frac{3.1255}{x} = \frac{7.86}{6.68}$ $x = 2.6583$

ORIGINAL PAGE IS
OF POOR QUALITY

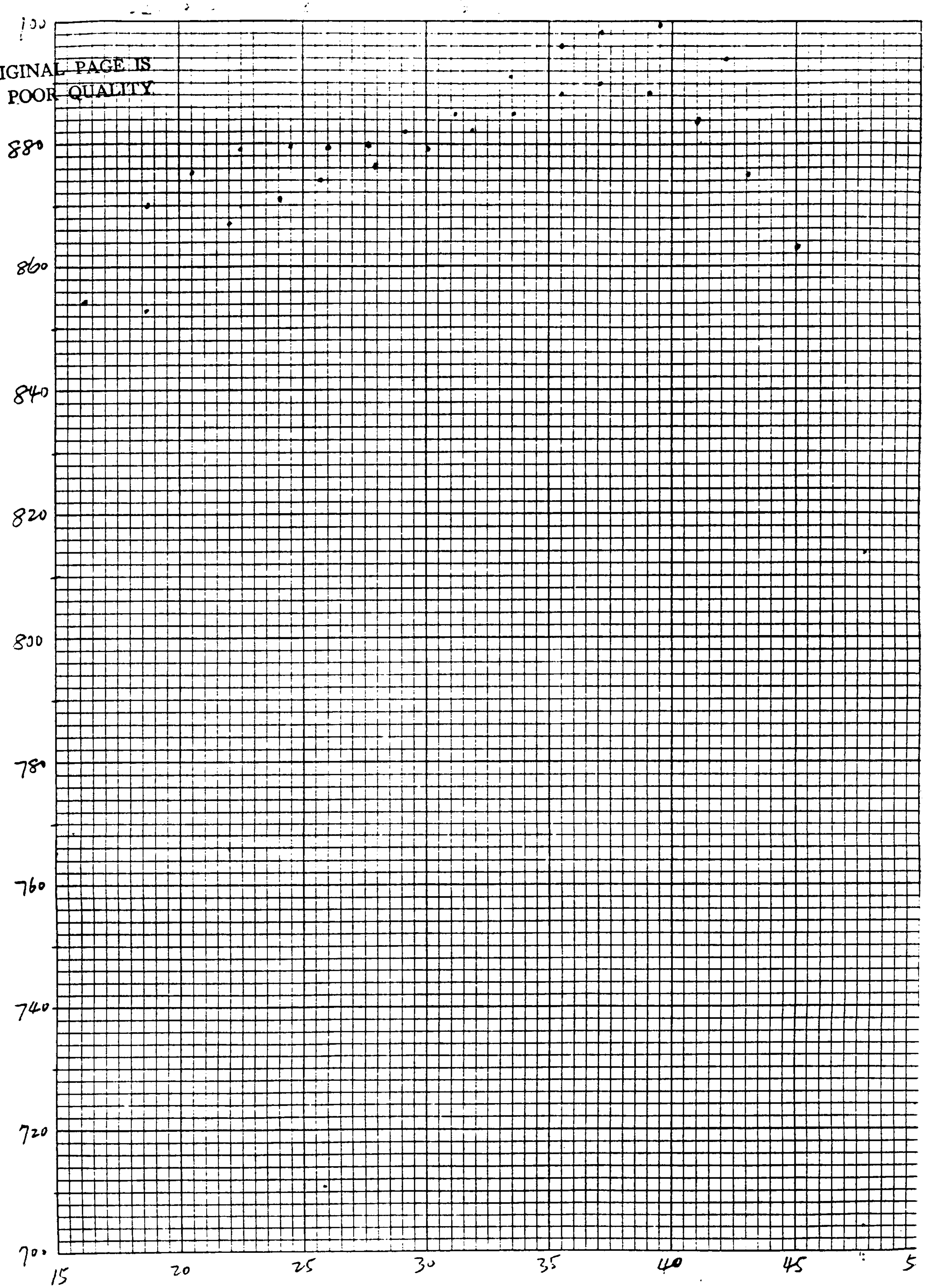

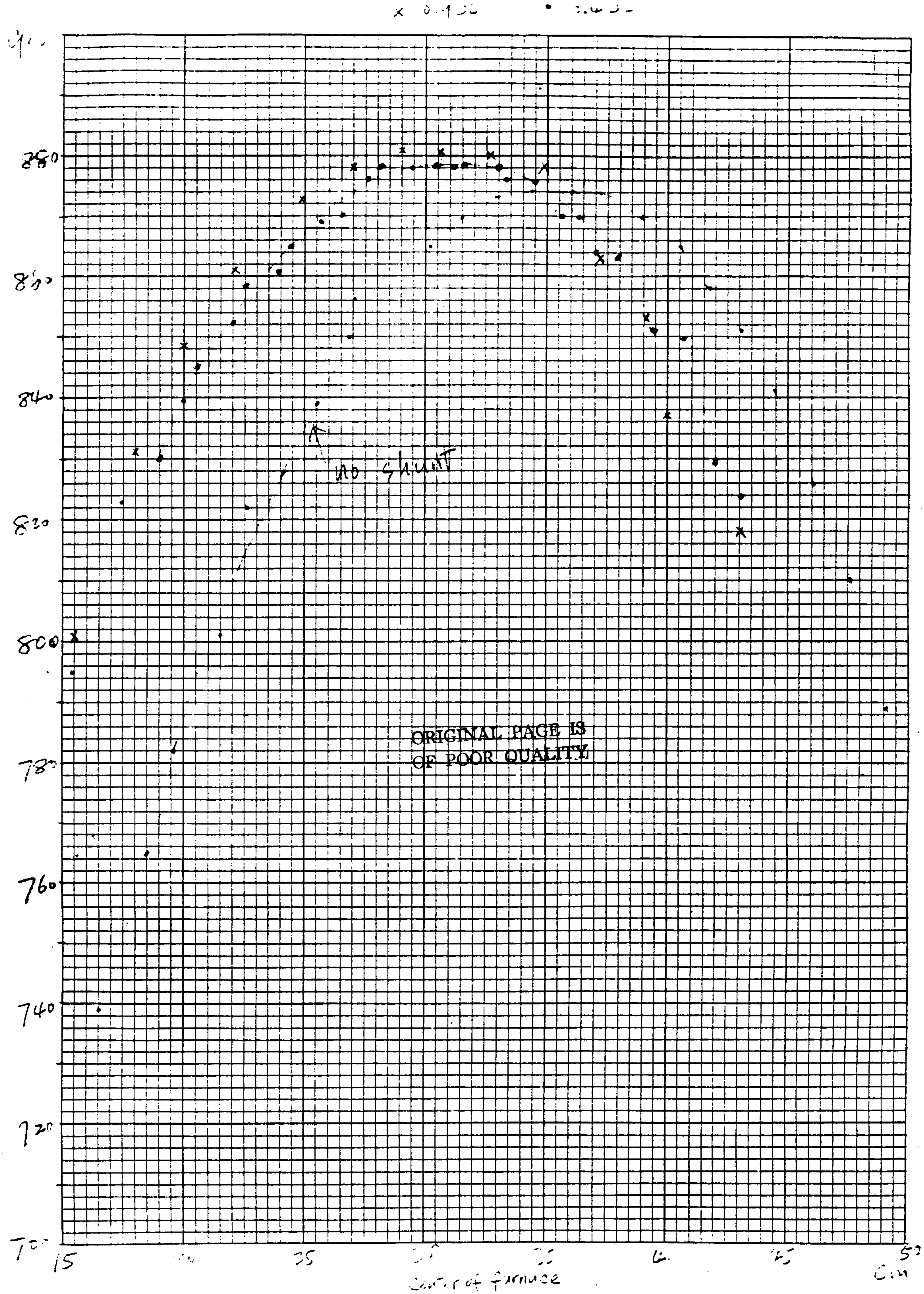
880
860
840
820
800
780
760
740
720
no shunt
15
25
50
Center of furnace
cm

ORIGINAL PAGE IS
OF POOR QUALITY

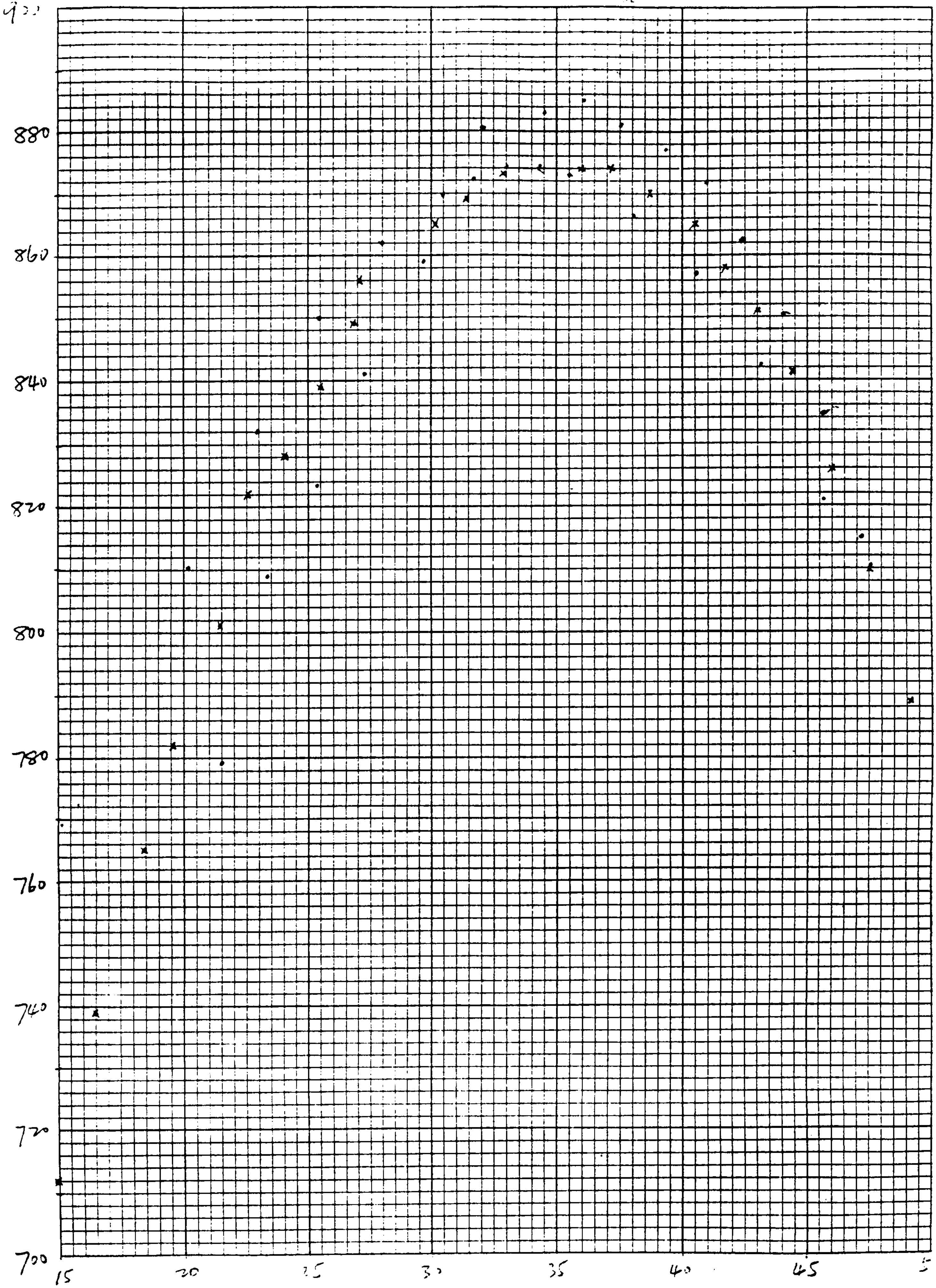

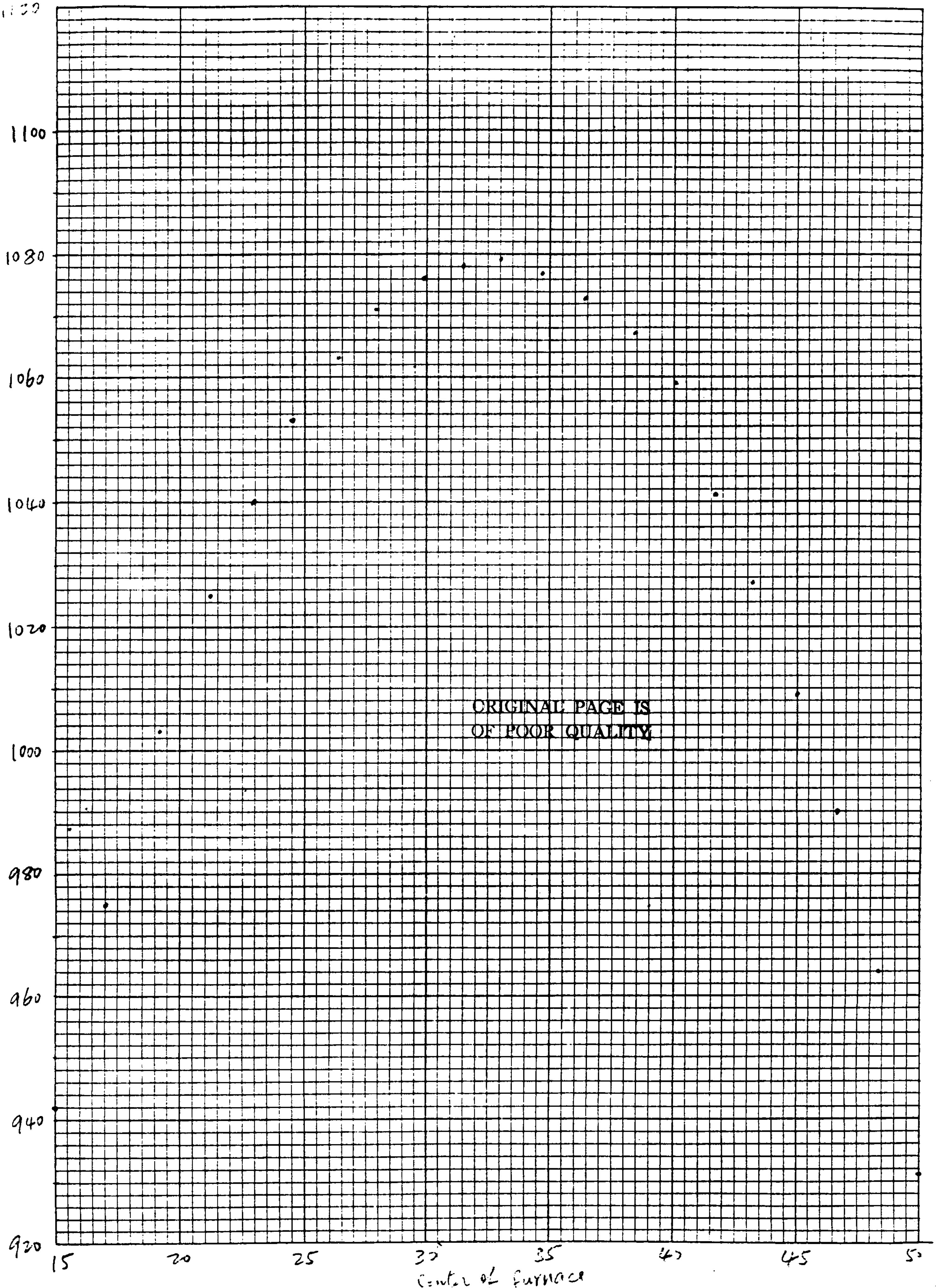
1100
1080
1060
1040
1020
1000
980
960
940
920
15
20
25
35
45
Center of furnace
ORIGINAL PAGE IS
OF POOR QUALITY

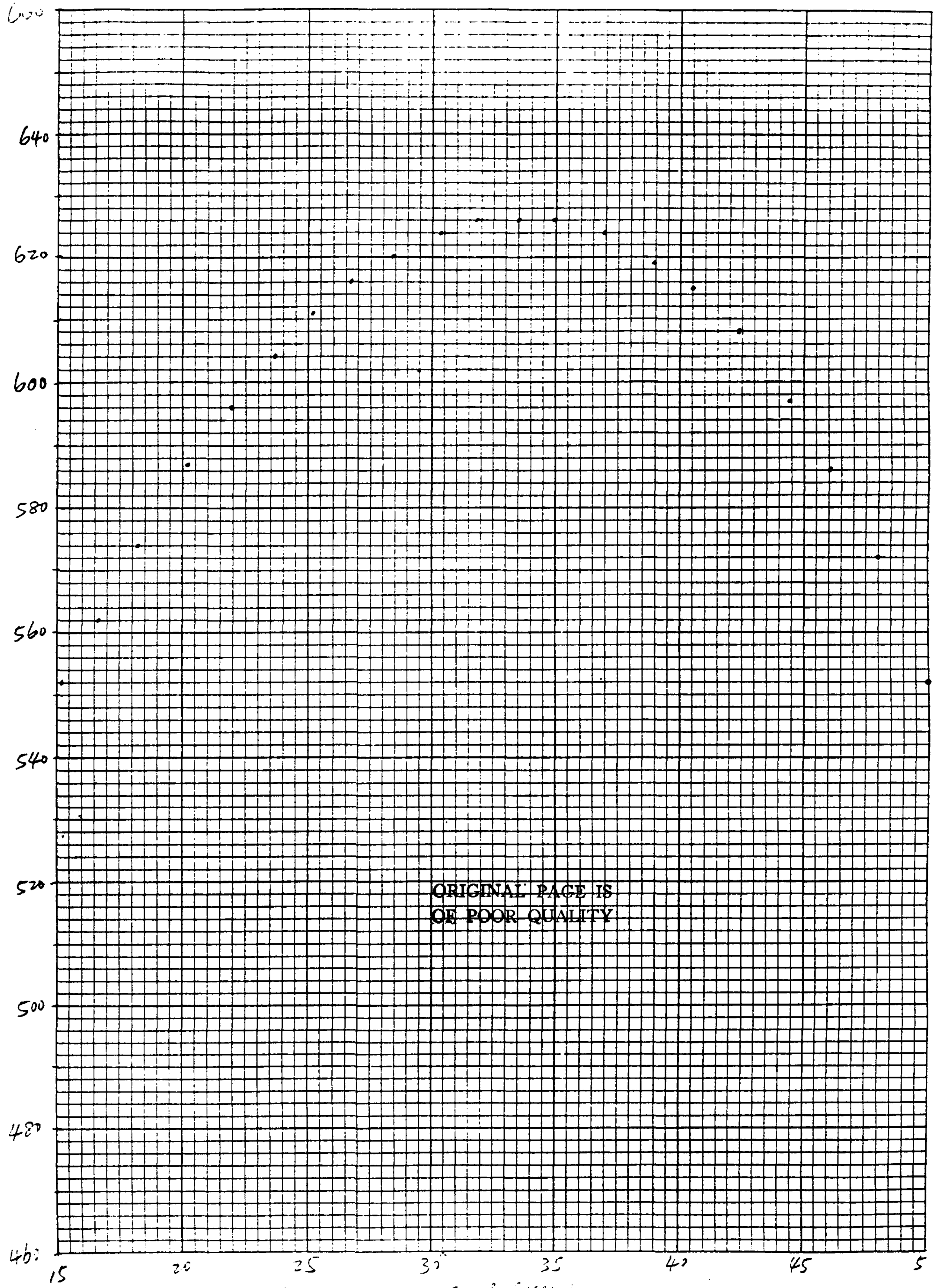
660
640
620
600
580
560
540
520
500
480
460
15
20
25
30
35
40
45
5
ORIGINAL PAGE IS
OF POOR QUALITY

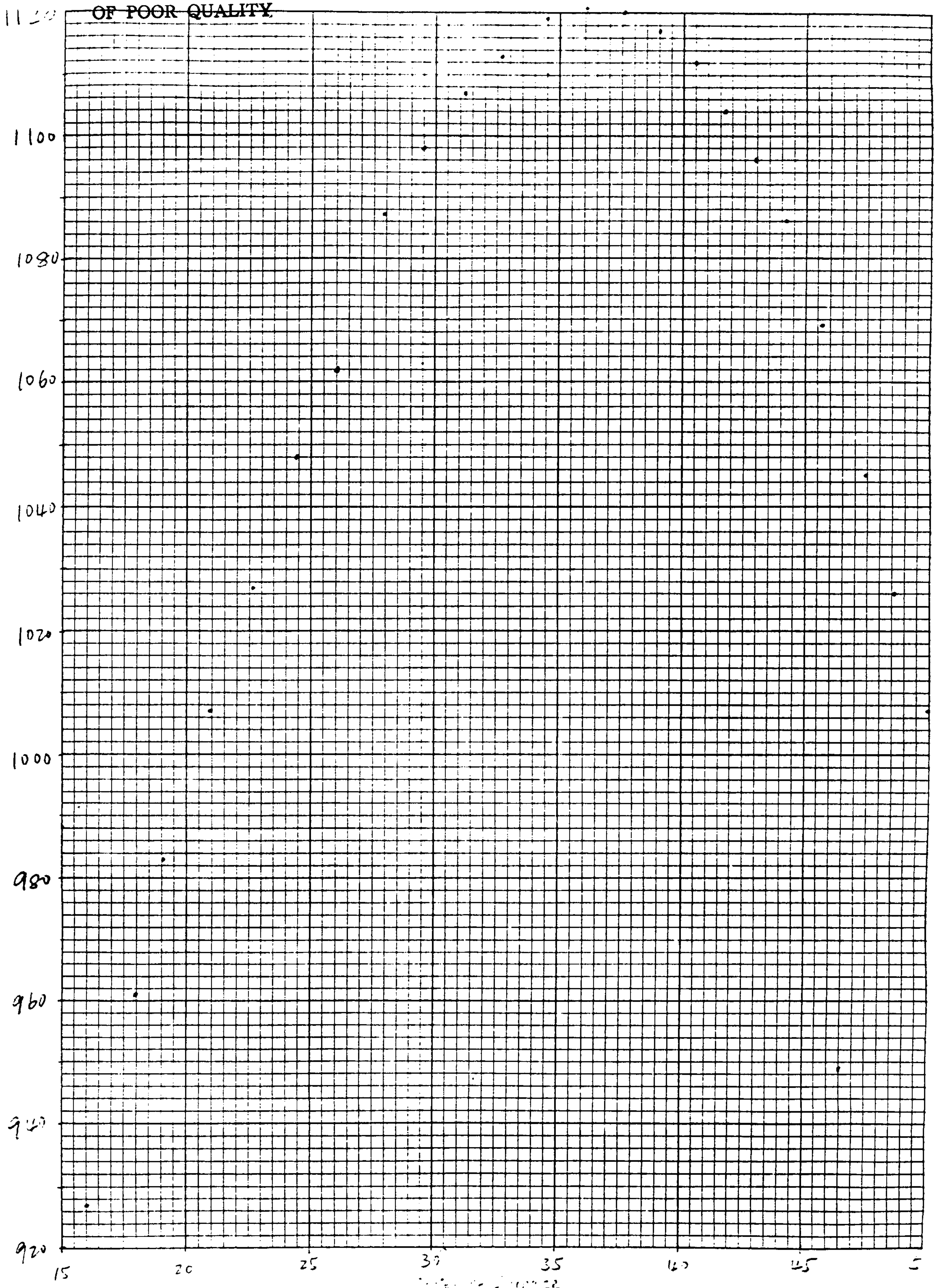
1100
1080
1060
1040
1020
1000
980
960
920
15
25
35

Type K

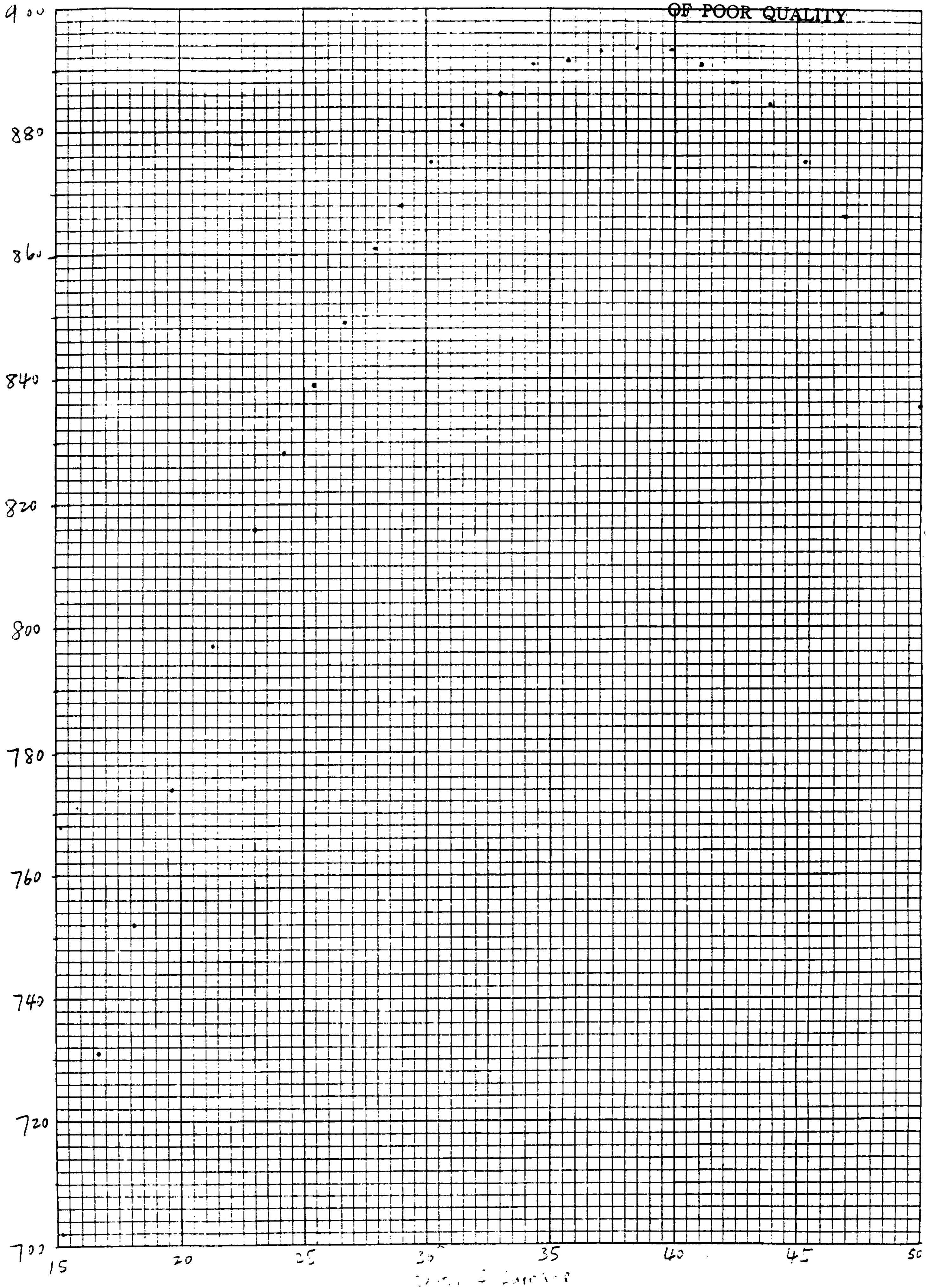

ORIGINAL PAGE IS
OF POOR QUALITY

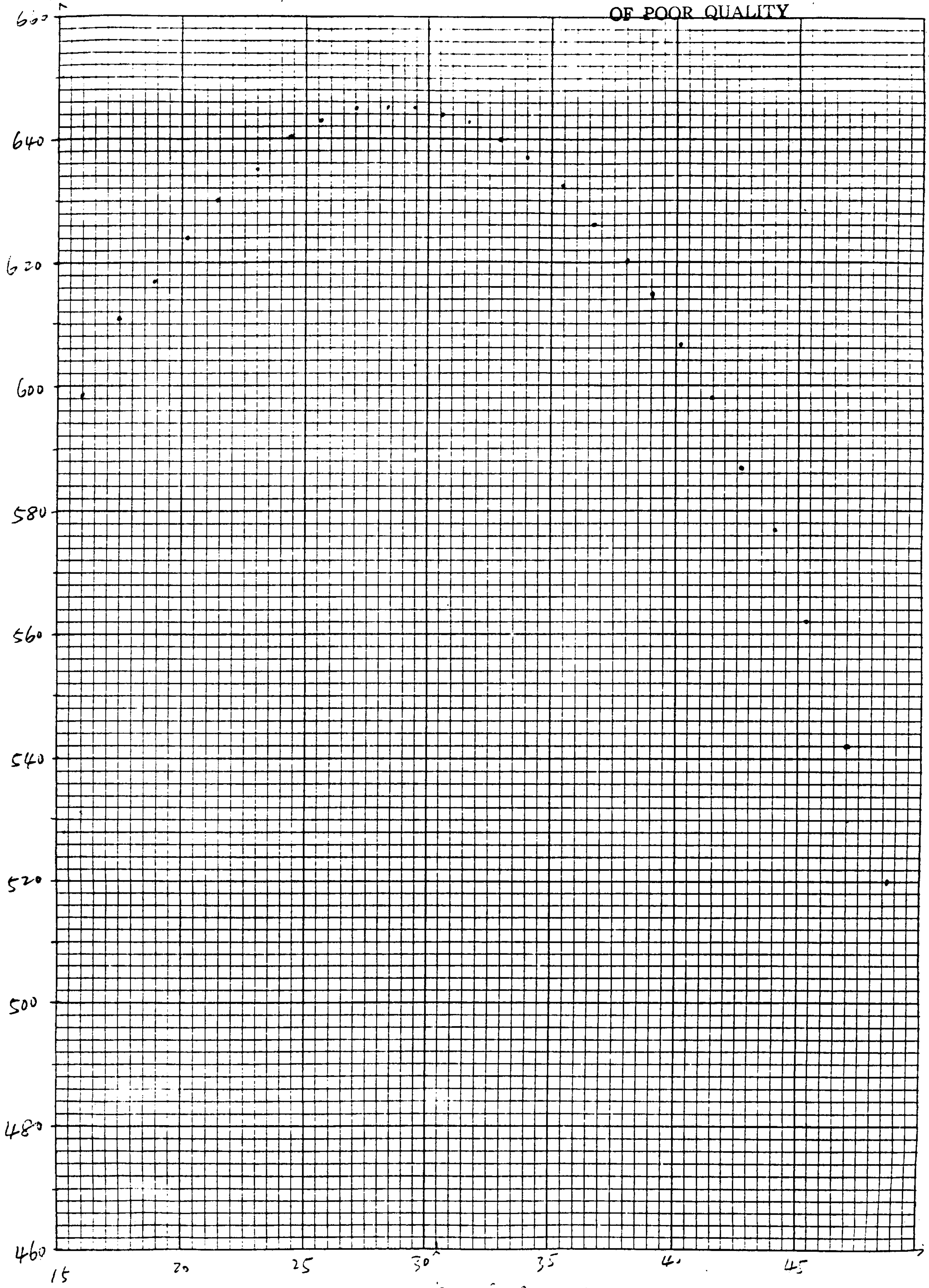

CONVECTION IN A VERTICAL AMPOULE DUE TO NON-AXISYMMETRIC TEMPERATURE DISTRIBUTION

J. Iwan D. Alexander, Jalil Ouazzani and Franz Rosenberger
Center for Microgravity and Materials Research
University of Alabama in Huntsville

1. Introduction

Convection and segregation in directional solidification and crystal growth by the Bridgman-Stockbarger technique have been traditionally treated by assuming axisymmetric thermal conditions on the ampoule wall. For most recent work and earlier references see [1]. It is, however, difficult to achieve such a condition in an experimental setup. Conventional heating devices (furnaces) typically have several degrees asymmetry in the temperature distribution of a plane normal to the geometrical symmetry axis. This can be significantly improved upon using heat pipes. But the Bridgman technique requires axial temperature gradients, i.e. transition zones between two quasi-isothermal zones (heat pipes) at different temperatures. Furthermore the temperatures required for the melt growth of most technologically important materials are high enough that radiative heat transfer to the ampoule is significant, if not dominant. Then, any axial misalignment of the ampoule, even in a perfectly axisymmetric gradient, will lead to a non-axisymmetric temperature distribution on the ampoule wall. This is due to the different view factors of the ampoule surface elements in a plane normal to the ampoule's axis.

Any deviation from an axisymmetric temperature field on the wall of a vertical ampoule represents a horizontal temperature gradient. The **horizontal density gradient** that results from thermal expansion in the melt under this condition **must lead on Earth to** some bouyancy-driven **convection,** no matter what the axial (vertical) temperature distribution that is imposed on the melt. It is the purpose of this study to estimate the magnitude of such convective flows for conditions representative of the MSFC mercury-cadmium-telluride (MCT) Bridgman setup.

2. Model and Method of Solution

The model consists of a closed vertical cylinder of radius R=0.25cm and height H=0.5cm. A vertical, convectively stabilizing temperature difference of 4.4 °C is imposed on the cylinder with the temperatures of the lower and upper plates, respectively, being kept constant at T_1=958.1 and T_2=962.5 °C.

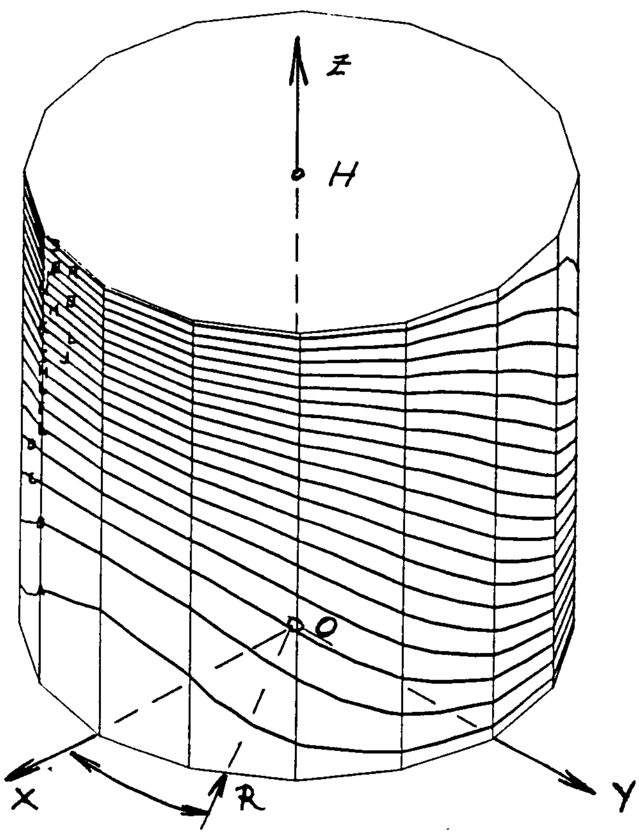

(a)

TABLE 1

Location	Temperature [°C]
A	958.115
B	958.346
D	958.807
E	959.038
F	959.268
G	959.499
H	959.729
I	959.959
J	960.190
K	960.420
L	960.651
M	960.882
N	961.112
0	961.343
P	961.573
Q	961.804
R	962.034
S	962.265
T	962.497

(b)

Fig. 1. Defining sketch. (a) Coordinate system and wall temperature (isotherms) distribution. (b) Table of temperature values for isotherms in (a).

On the side wall, as depicted in Fig. 1, a temperature distribution of the form

$$T_{wall} = T_1 + (T_2 - T_1)\frac{zR}{H}\left(1\text{-}\cos\left(\frac{\pi\, z}{2H}\right)\cos\theta\right)$$

is imposed. This amounts to a maximum horizontal temperature difference of 2.2 °C. The cylinder is completely filled with a fluid of Prandtl number $Pr=10^{-2}$ (or thermal diffusivity $\kappa = 1.3\text{x}10^{-1}$ cm^2/sec and kinematic viscosity $\nu=1.3\text{x}10^{-3}$ cm^2/sec) and thermal expansion coefficient $\beta = 2.45\text{x}10^{-4}$ K^{-1}. These parameter values are representative of molten germanium [1]; corresponding values for MCT alloys are, unfortunately, not known with sufficient accuracy at this point. The acceleration of gravity is assumed to act downward, parrallel to the cylinder axis. For simplicity, its value is assumed to be $g=10^3$ cm/sec^2.

It is assumed that the melt behaves as a Boussineq fluid. The basic equations governing the transport of momentum and heat are then

$$\frac{\partial \mathbf{u}}{\partial t} + (\text{grad } \mathbf{u})\mathbf{u} = -\frac{1}{\rho_o}\text{gradp} + \nu\Delta\mathbf{u} - \frac{\Delta\rho}{\rho_o}g\mathbf{k}, \tag{1}$$

$$\text{div } \mathbf{u} = 0, \tag{2}$$

$$\frac{\partial T}{\partial t} + \mathbf{u} \bullet \text{gradT} = \kappa\Delta T, \tag{3}$$

where $\mathbf{u}$, p, and T are the fluid velocity, reduced pressure and temperature, ν is the kinematic viscosity, ρ_o is the (constant) reference density, $\mathbf{k}$ is the unit vector in z-direction and $\Delta\rho/\rho_o$ is the change in density due to temperature. On the boundaries we impose, in addition to the above thermal conditions, the no-slip condition $\mathbf{u} = 0$.

The system of equations (1-3) was solved for these boundary conditions employing the finite element code FIDAP [2,3]. The computational domain was discretized with the mesh of 8 node bricks depicted in Fig. 2. The non-isometric grid in physical space was transformed to a grid of isoparametric bricks in logic space. For each of these elements the velocity components and the temperature were approximated using trilinear interpolation functions. The pressure was approximated using a piecewise constant discontinuous pressure approximation (penalty method)[4]. For the steady-state algorithm we used a Newton-Raphson method combined with Quasi-Newton updating [5,6].

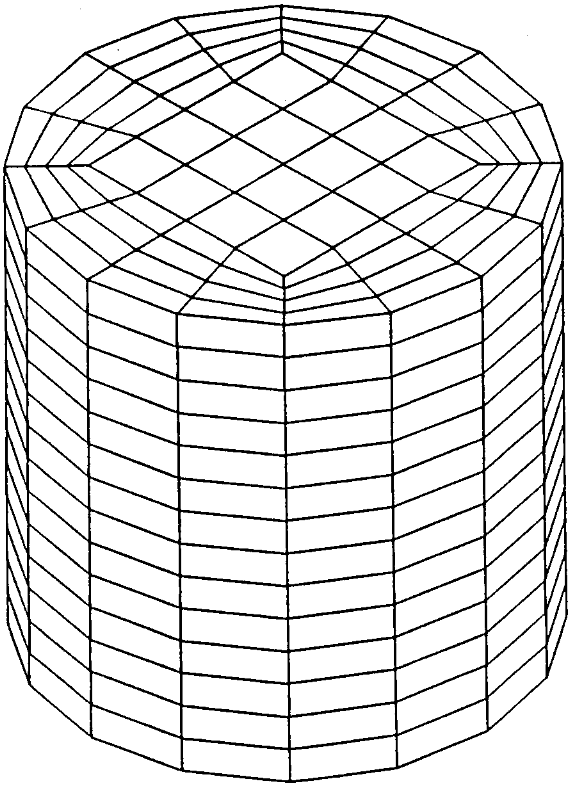

Fig.2. Mesh system used for finite element solution.

3. Results

The major result of our modelling is that the imposed temperature distribution leads to convective flow of significant strength. As illustrated by the velocity field in the symmetry plane (y=0) presented in Fig. 3a, one convective roll is established. Note that the maximum velocity magnitude is in excess of 0.25 cm/sec. Figure 3b shows the resulting temperature distribution in the symmetry plane. The flow has strong three-dimensional features, as is illustrated by the velocity plots for various cross-sectional planes that are presented in Figs. 4-6 together with the corresponding temperature distributions. Note that the velocities in all these cross-sections are of comparable magnitude.

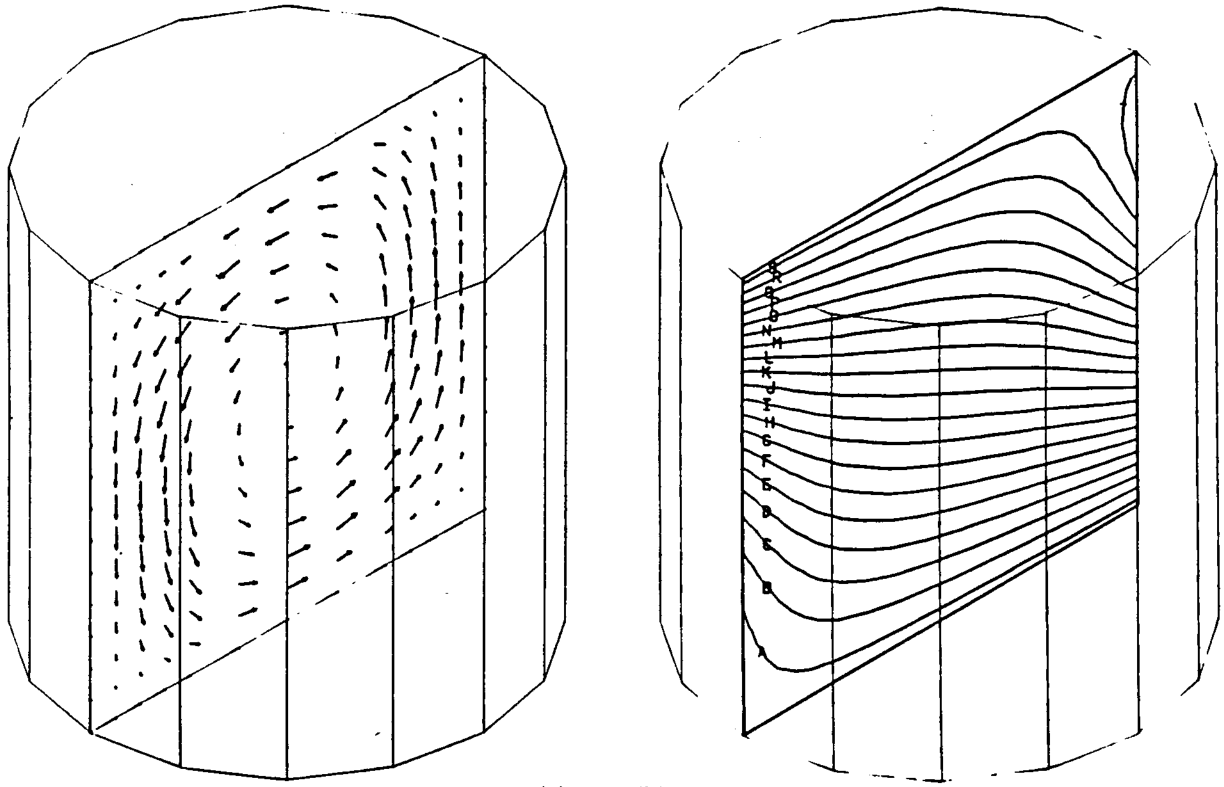

(a) (b)

Fig.3. (a) Velocity field and (b) temperature distribution (isotherms, for values see Table 1) in symmetry plane (y=0). Maximum vector plotted corresponds to 0.27 cm/sec.

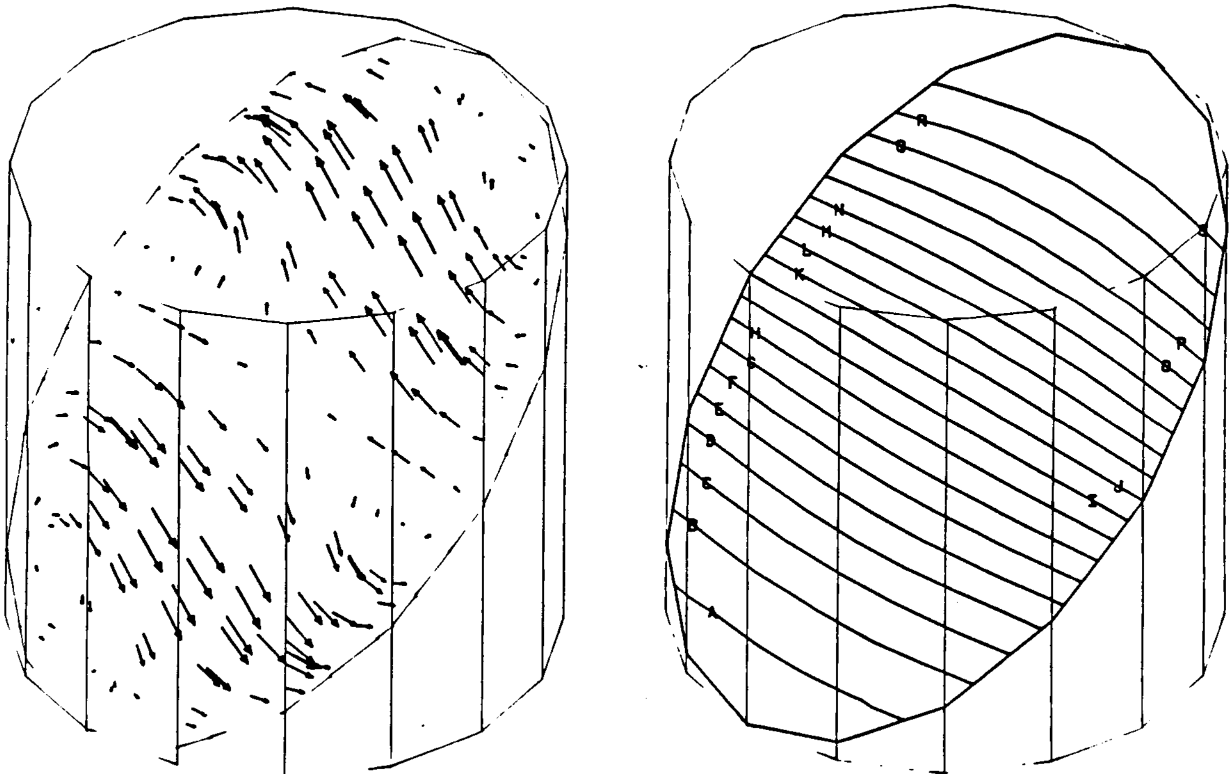

(a) (b)

Fig.4. Plane z=H/2 - x. (a) Velocities at points in plane. Maximum vector plotted corresponds to 0.22 cm/sec. (b) Isotherms; for values see Table 1.

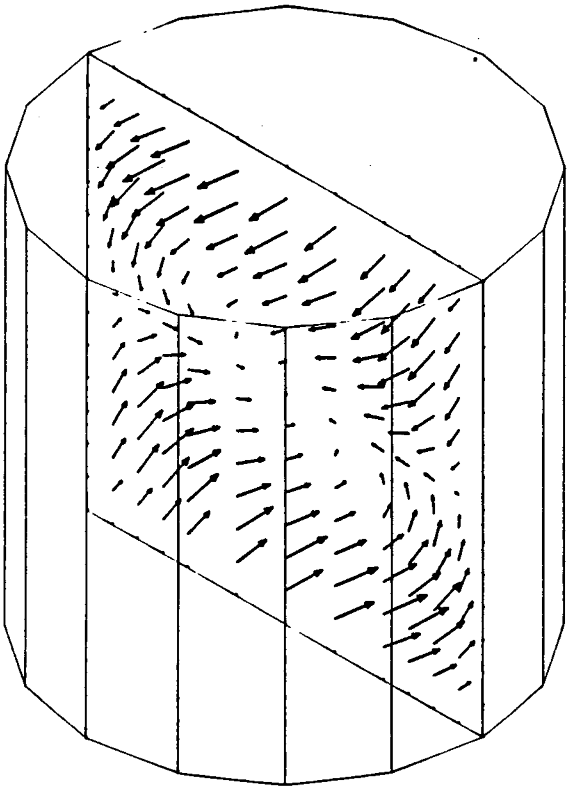

(a)

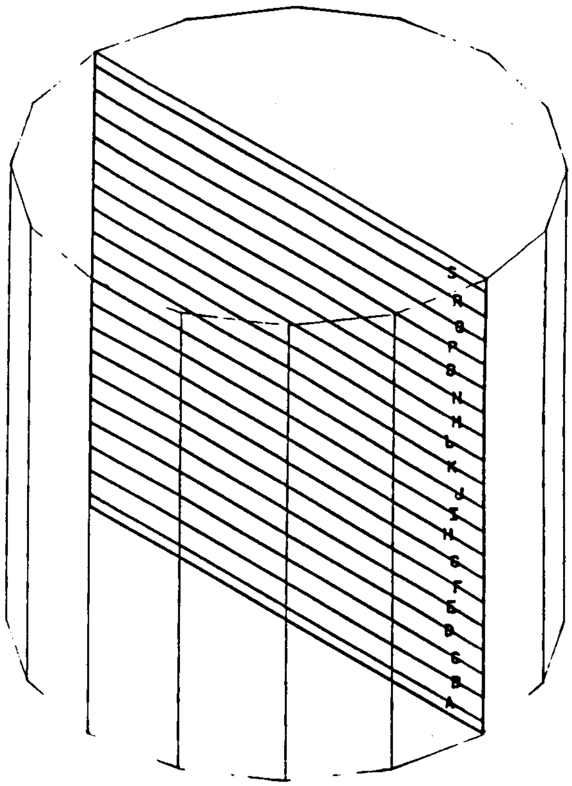

(c)

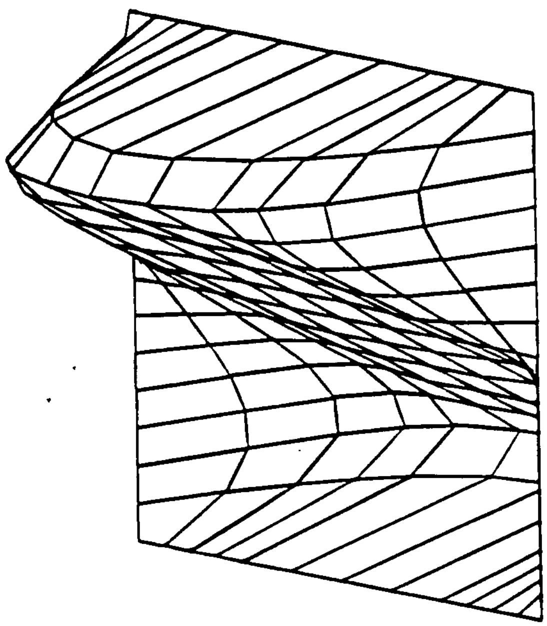

(b)

Fig.5. Plane x=0. Velocities at points in plane. (a) Vector representation, (b) velocity surface. Maximum vector plotted corresponds to 0.23 cm/sec. (c) Isotherms in plane; for values see Table 1.

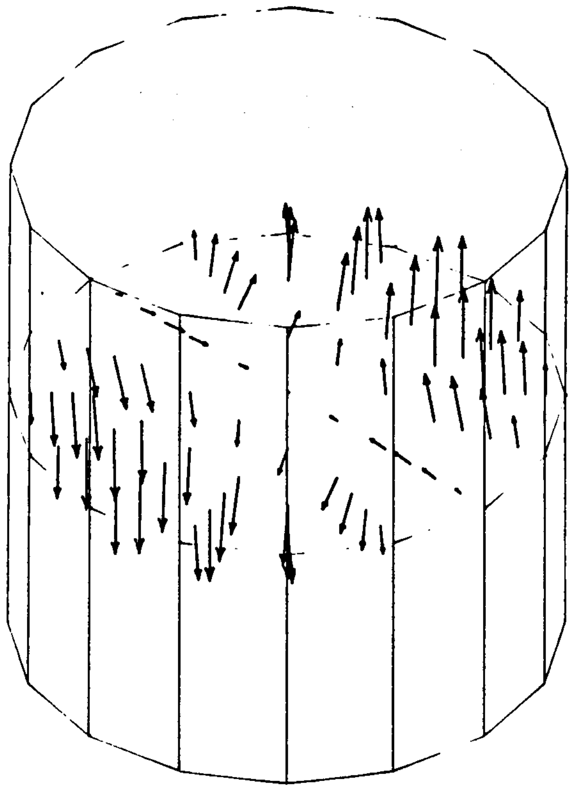

(a)

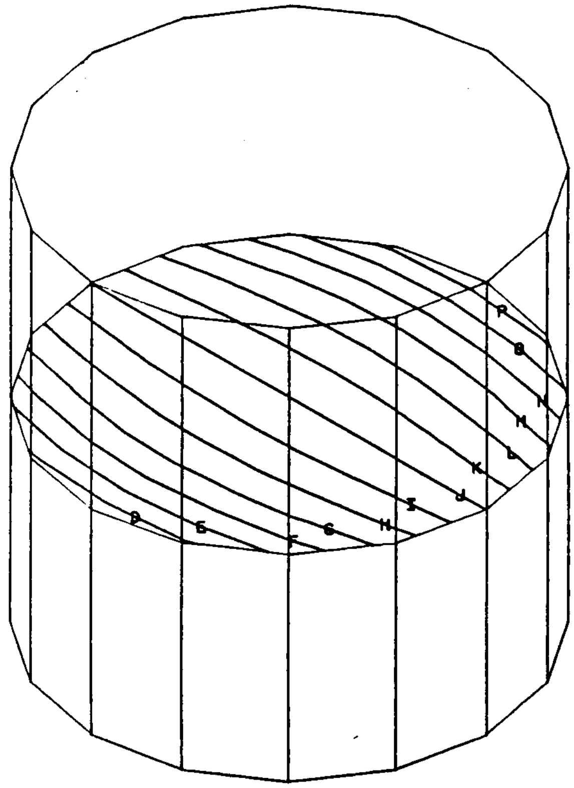

(c)

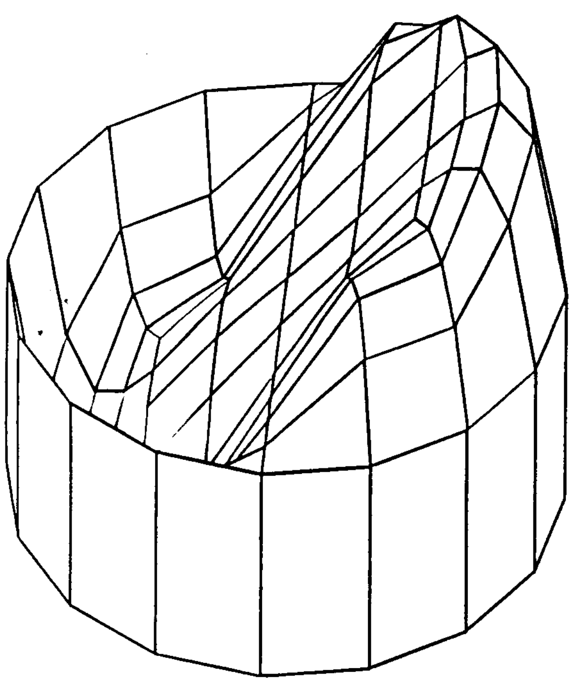

(b)

Fig.6. Midplane z = H/2. Velocities at points in plane; (a) vector representation, (b) velocity surface [rotated -45° with respect to (a)]. Maximum vector plotted corresponds to 0.27 cm/sec.
(c) Isotherms; for values see Table 1.

4. Discussion and Conclusions

In view of the astounding magnitude of the convective velocities obtained, we have used the basic solution of Hart's sideways diffusion model (setting the solutal gradient to zero) to calculate the maximum velocity associated with a horizontal temperature difference maintained between two vertical planes [7]. One would expect that Hart's model, due to less flow impedance by no-slip surfaces, results in a somewhat larger convection velocity than our totally confined geometry. This expectation was, indeed, confirmed by the value of 0.83 cm/sec that we obtained for the maximum velocity, as compared to 0.27 cm/sec from our cylindrical model for otherwise similar conditions.

It should be emphasized that such high convection velocities that result from "small" deviations from axisymmetric thermal boundary conditions, exceed diffusion velocities characteristic of semiconductor melts by some three orders of magnitude. These convection velocities also exceed those obtained in earlier Bridgman modelling work (Grenoble furnace) [1], assuming axisymmetry, by one to two orders of magnitude. In addition, the convective flow resulting from the asymmetry condition extends throughout the melt. This is in contrast to the highly localized, interfacial flows obtained in the earlier modelling. These localized flows arise from the mismatch of the thermal conductivities of melt, crystal and container.

Our preliminary study needs to be expanded considerably. For instance, the stabilizing effect of larger vertical temperature gradients needs to be explored. Furthermore, the effect of reducing the severity of the asymmetric thermal boundary condition needs to be investigated by imposing flux conditions rather than a fixed temperature profile. But is it probably safe to say, even at this early point, that our model shows that symmetric transport conditions in the Bridgman technique will be very difficult to realize in the laboratory practice. Future modelling must recognize this.

5. References

[1] P.M. Adornato and R.A. Brown, J. Crystal Growth, **80** (1987) 155.

[2] M.S. Engelman, FIDAP Fluid Dynamics Analysis Program User/Theoretical Manual, Control Data Corporation, Pub. No. 84003650 (1983).

[3] M.S. Engelman and R.L. Sani, Proceedings of the ASME Convection in Enclosures Conference (1983).

[4] M. Bercovier, Ph.D. Dissertation, University of Rouen (1976).

[5] H. Matthies and G. Strang, Int. J. Num. Meth. Eng. **11** (1977) 1155.

[6] J. Dennis and J. More, SIAM Rev. **19**, (1965) 46.

[7] J. E. Hart, J. Fluid Mech. **49** (1971) 279.